

# Laminar Flow Vortex Shedding Around the Cylinder

Alsheikh Ali  
*FOSSEE Team, IIT Bombay*

## Synopsis

This research migration project presents the results of numerical modeling of Karman vortex shedding laminar flow generation performed with OpenFoam package application. The influence of the mechanical elements located downstream of the bluff body on the vortex frequency. Two various geometrical configurations have been applied. Considerable differences in pictures of distributions of pressure, horizontal and vertical velocities have appeared for various configurations. Qualitative as well as quantitative results are presented in the report. They confirm the significant dependence of the Karman vortex street parameters on the meter configuration.

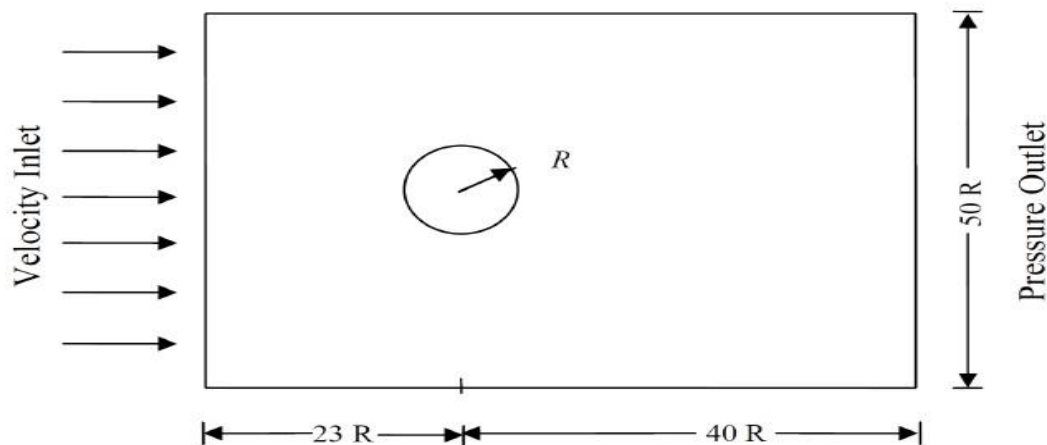


Figure 1: Geometry and Dimensions

dimensions of the geometry stated in the figure 1 are:  $L = 63m$ ,  $H = 50m$ ,  $R=1m$ .  
Flowing fluid is entering from the inlet with a velocity of  $1m/s$  and exiting from the outlet.

## References

G. Pankanin, "Simulation of influence of mechanical elements on Karman vortex street parameters," International Journal of Electronics and Telecommunications, vol. 65, no. 2, pp. 229–234, 2019, doi: 10.24425/ijet.2019.126305.

## 1 Introduction

Flow around a cylinder is a classic problem in fluid mechanics. It is a problem of practical importance. Off shore structures, bridge piers, single silos, and to some extent cooling towers are typical cases where we face flow over cylindrical structures [1]. Vortex shedding is an important phenomenon that occurs in flow around these types of structures for a wide range of Reynolds numbers [2]. The frequency of vortex shedding and analysis of vortex induced vibrations play an important role in the design of these structures. In this report, laminar flow around a cylinder is simulated using OpenFOAM and the results are validated by comparing them with experimental data [3]. First of all, the physical aspect of flow around a cylinder is reviewed. The numerical aspects of simulating the case together with the case set up in OpenFoam are discussed.

## 2 Governing Equations and Models

Using discretization schemes the Navier-Stokes equations are transformed from partial differential equations to algebraic equations. Different schemes are available to discretize convection, diffusion, and gradient terms. They have different properties in terms of accuracy and stability and should be chosen properly for the specific problem. First order schemes are in general too diffusive and would underpredict forces and gradients.

### 2.1 Navier Stokes Equations

Already in 1755, Leonard Euler proposed [4] a system of partial differential equations describing fluid motion. There were based on assumption that fluid can be treated as a body of a continuous structure. In such a body there appear the forces proportional to mass elements of the fluid (mass forces) and forces proportional to surface elements (surface forces). It is worth mentioning, that Euler introduced the pressure term. So, Euler applied the Newtonian mechanic for the description of phenomena appearing in fluids. He also developed mathematical methods for the solution of a mechanic of fluids problems. Several dozen years later M. Navier in [5] and G.G. Stokes in [6] completed Euler's equations taking into account the fluid viscosity. Hence the name Navier – Stokes equations. In literature, these equations can be found in various forms. In the most common approach for non-compressed fluids, they may be presented as:

$$\rho \cdot \frac{dV}{dt} = \rho \cdot F - \text{grad}(p) + \mu \cdot V \quad (1)$$

and for compressed fluids:

$$\rho \cdot \frac{dV}{dt} = \rho \cdot F - \text{grad}(p) + \text{div}(\mu \cdot \Delta M) \quad (2)$$

Where,

$\rho$	fluid density
$V$	velocity vector
$A$	mass force vector
$P$	pressure
$M$	viscous strain tensor
$\mu$	dynamic viscosity

## 2.2 Force Coefficients

Force Coefficients: calculates lift, drag, and pitching moment coefficients for a patch list. These coefficients are defined as:

$$C_l = L / (0.5 \rho A U_\infty^2) \quad (3)$$

$$C_d = D / (0.5 \rho A U_\infty^2) \quad (4)$$

$$C_M = M / (0.5 \rho A U_\infty^2) \quad (5)$$

Where,

$C_l$	Lift coefficient
$C_d$	Drag coefficient
$C_M$	Moment coefficient
$\rho$	fluid density
$U_\infty$	Flow velocity
$D$	Bluff body diameter
$L$	Pipe length
$M$	viscous strain tensor
$A$	Bluff body cylinder Area

To calculate the coefficients the reference area and reference length (for moment coefficient) should be specified by the user. By definition, the lift force acts perpendicular to the velocity vector, and drag acts parallel to it. These directions as well as pitching moment direction are declared in the function block [7].

### 3 Simulation Procedure

Preprocessing mainly consists of preparing the blockMeshDict to generate the block structured mesh, setting the required boundary conditions in the 0 folder, and setting the parameter in the controlDict file. Simulate and solve the governing PDEs. In the following, the steps towards the simulation of laminar flow around a cylinder are explained. The schematic of the problem is shown in figure 2.1



Figure 2: Tested configurations

#### 3.1 Geometry and Mesh

The mesh can be generated using different blocking strategies. Here we use blocks to generate an o-grid type mesh around the cylinder. Using blockMesh utility, geometry, and mesh defined with 5th blocks for case A and 12th blocks for case B, are to the o-grid mesh to extend the domain in the downstream region of the flow, the first two numbers indicate the start and endpoint of the arc [8]. Infinite number of circular arcs can be defined between two points, we need a third point to specify the exact arc we need. The coordinate of this third point follows after start and endpoint numbers in the arc command in both these cases. There are other options for defining curved edges between vertices. Using splines, for example, one can represent an airfoil profile using just 3 vertices and defining 3 splines for edges connecting them. Available options for defining curved edges in blockMeshDict are arc, simpleSpline, PolyLine, and polySpline. Their description is available in OpenFOAM user guide. The schematic of the Mesh is presented in figure 3 and 4.

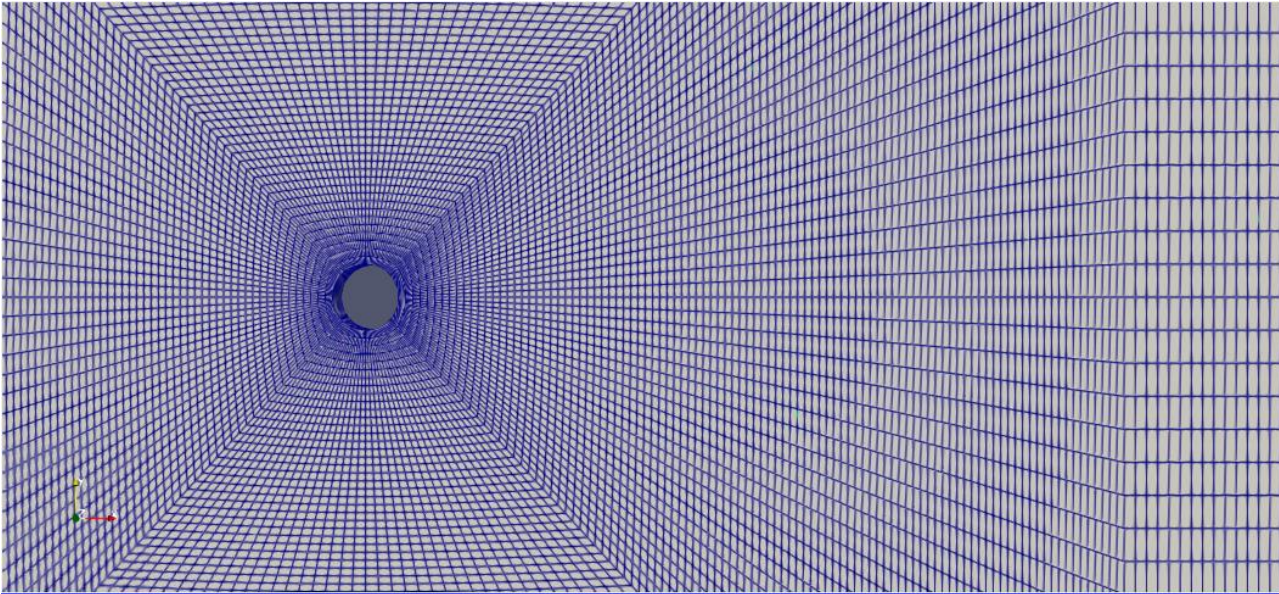


Figure 3: Schematic Mesh Case A

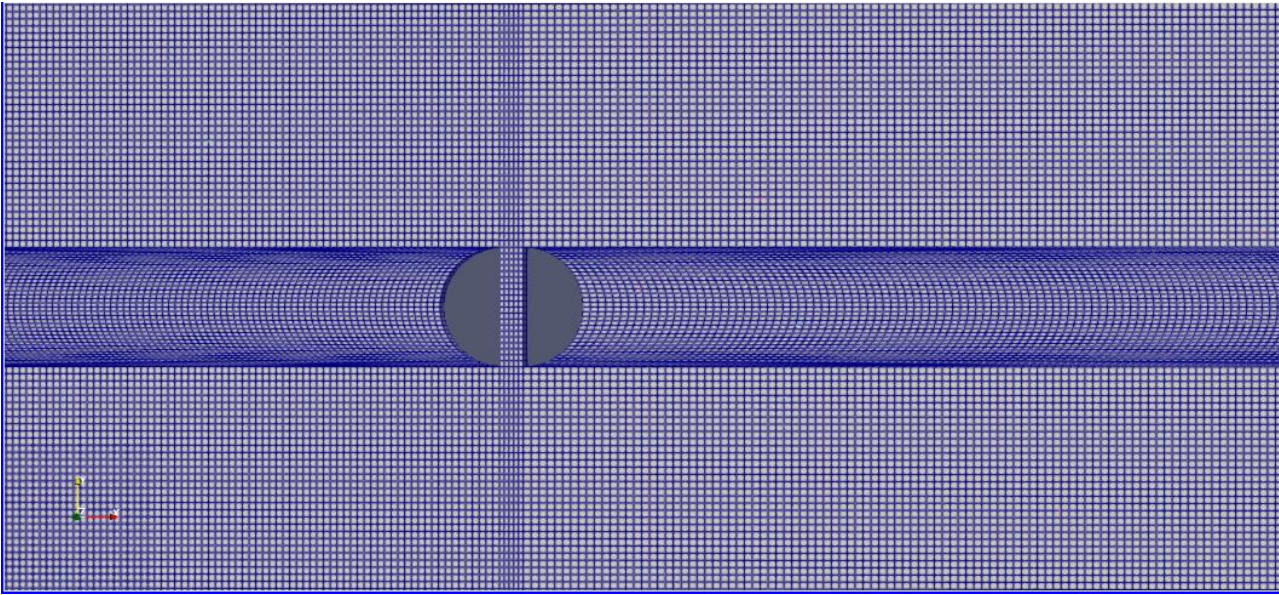


Figure 4: Schematic Mesh Case B

### 3.2 Initial and Boundary Conditions

Six patches are defined in this problem. Inlet, outlet, top, bottom, cylinder, sides. Top and bottom patches are defined to be far enough from the cylinder, they are defined as slip walls. Since it is a 2D problem, sidewalls are defined in a single patch with type empty. The boundary conditions used are summarized in table 2.1 The zeroGradient boundary condition implies the gradient to be zero normal to the patch and slip is the same as zeroGradient for scalar parameters while for vectors it implies fixedValue zero to the normal to the patch component of the vector and zeroGradient to tangential components of the vector. Other used boundary conditions are more or less self-explanatory. The magnitude of the velocity at the inlet is set to a fixed value of 1m/s, to fulfill  $Re = 100$  we can later play with dynamic viscosity.

Table 1: Boundary condition

Boundary Field	Velocity	Pressure
Inlet	fixedValue, uniform (1 0 0)	zeroGradient
Outlet	zeroGradient	fixedValue, uniform 0
Top	slip	zeroGradient
Bottom	slip	zeroGradient
Cylinder	fixedValue, uniform (0 0 0)	zeroGradient
Side	empty	zeroGradient

### 3.3 Solver

pisoFoam is a transient solver for incompressible flow. Both laminar and turbulent flows can be simulated using pisoFoam. It is based on the PISO algorithm, which stands for Pressure Implicit with Splitting of Operators, proposed by Issa in 1995[9]. It is a pressure-velocity coupling algorithm with a predictor step and two corrector steps. In the predictor step, the momentum equations are solved for an intermediate pressure field. The predicted velocity field at this stage does not satisfy the continuity condition. Then during the two predictor steps, velocity and pressure fields are corrected in a way to fulfill both, momentum and continuity equations [10]. The PISO algorithm consists of the following steps:

1. Prediction of the intermediate velocity field from momentum equations
2. PISO loop
  - i. Calculate mass fluxes on cell faces
  - ii. Solve pressure field (nNonOrtcorr times)
  - iii. Correct Velocity field
3. Repeat the PISO loop nCorr times
4. Solve the turbulence model
5. Proceed to the next time step

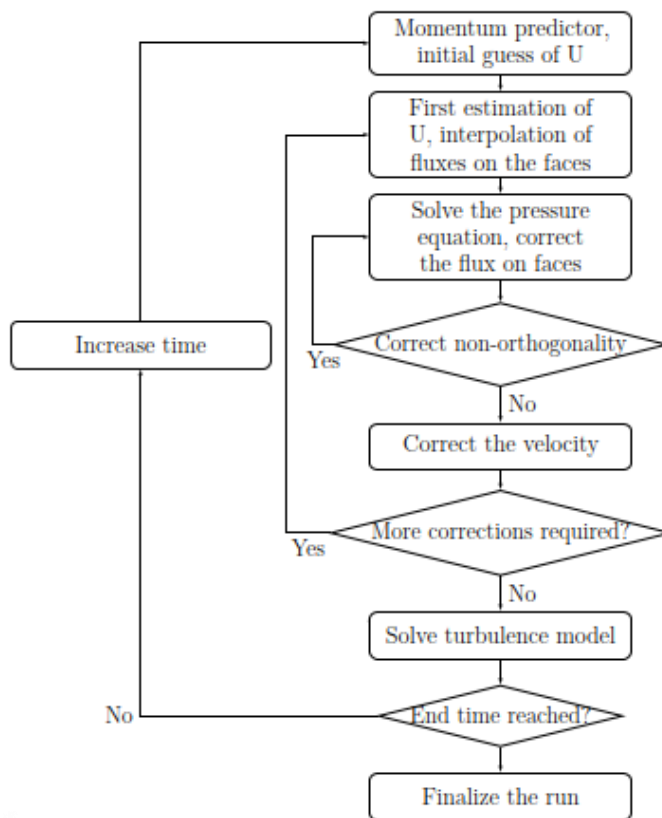


Figure 5: PISO algorithm steps

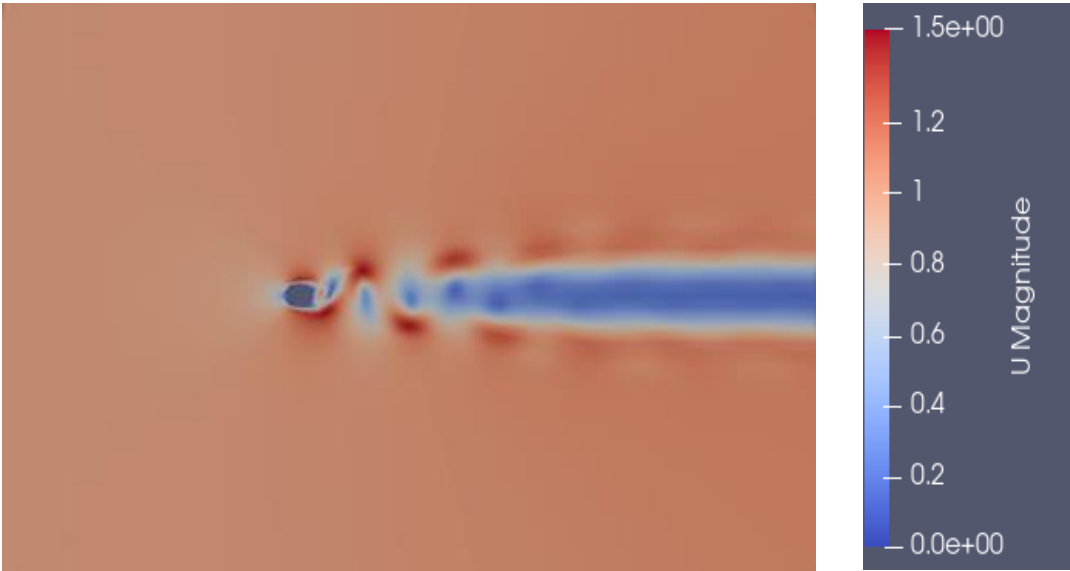


Figure 6: Velocity Magnitude Case A

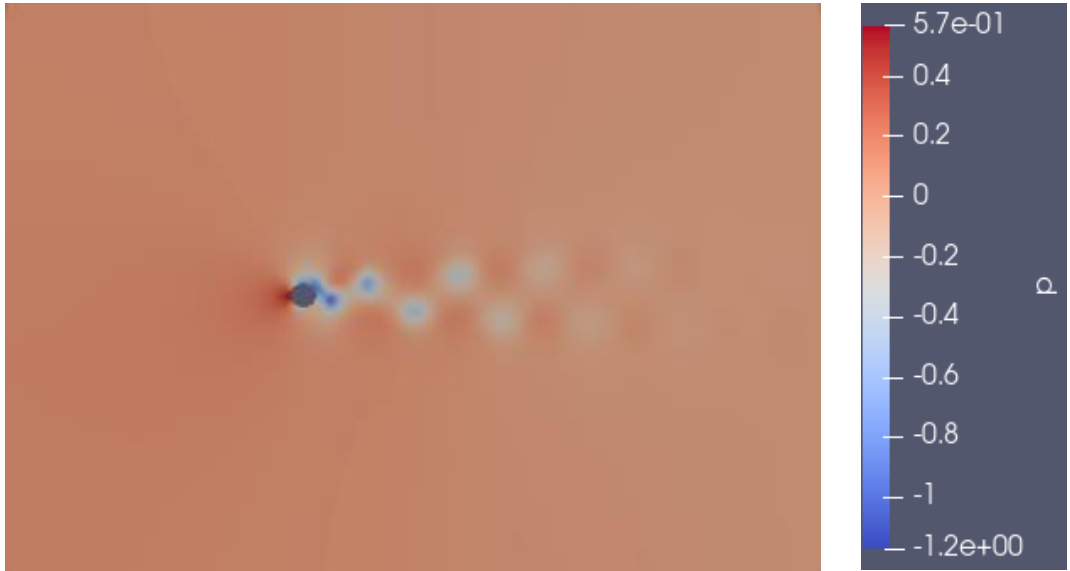


Figure 7: Pressure Case A

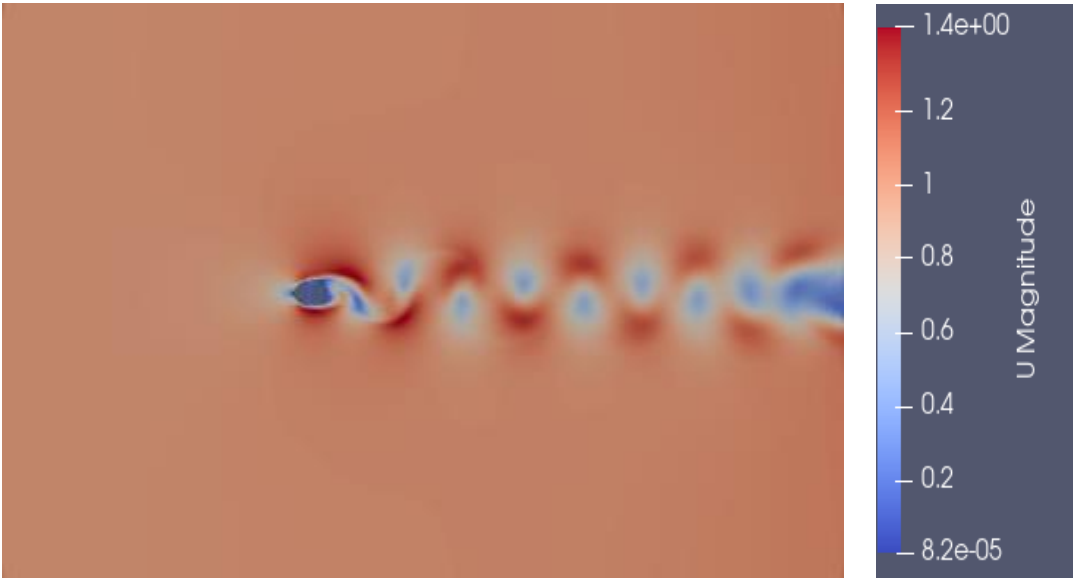


Figure 8: Velocity Magnitude Case B

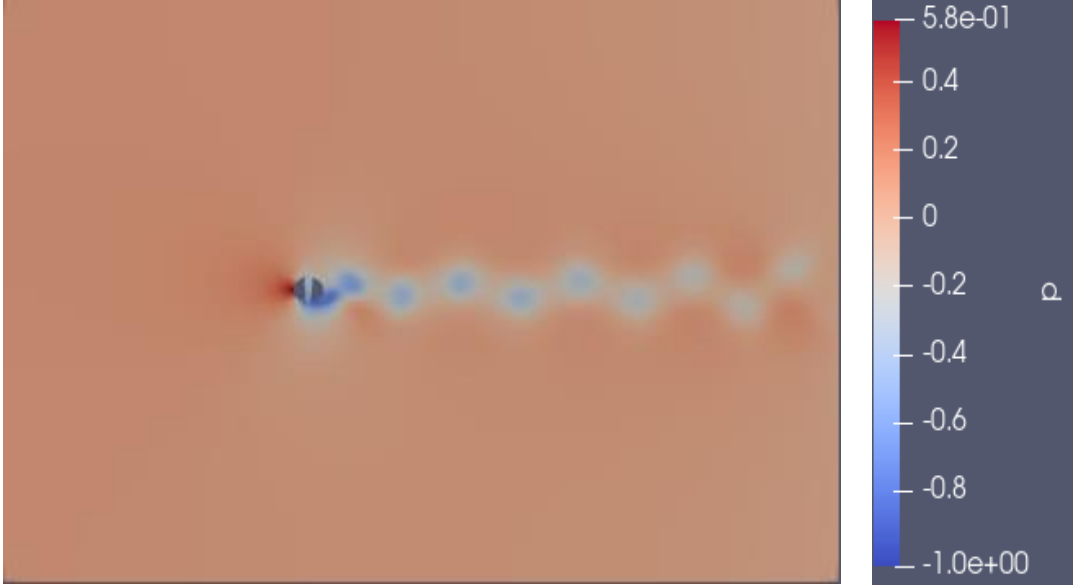


Figure 9: Pressure Case B

## 4 Results and Discussions

In this part, the results of the simulation are evaluated and compared with reference results reported in the literature. The initial flow needs some time to develop around the cylinder, what happens after a while is the onset of vortex shedding and development of the von Karman vortex street (figure 6,7,8,9). The Periodic shedding of the vortices into the wake results in an oscillating lift and drag force on the cylinder. The change in lift and drag coefficients in time can be seen in figures 10, 11, 12,13. With the emergence of vortex shedding and as flow develops itself around a cylinder the drag coefficient begins to oscillate about a mean value of 1.65 and 1.7. The amplitude of lift coefficient is 1.0 and 0.9. They are in a very good agreement with the reported values for drag coefficient and the amplitude of lift coefficient, and the plot residuals for both cases A and B is shown in figure14 & 15.

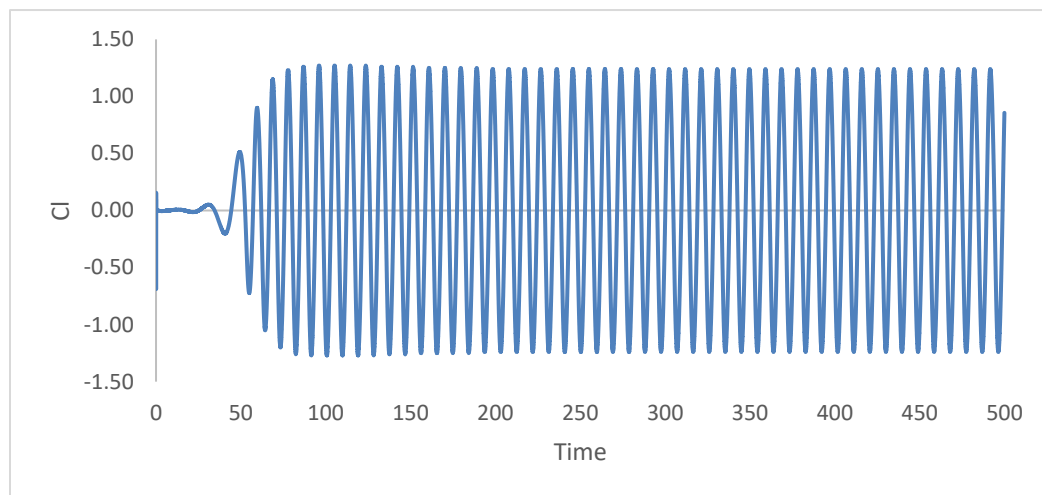


Figure 10: Lift coefficient Case A

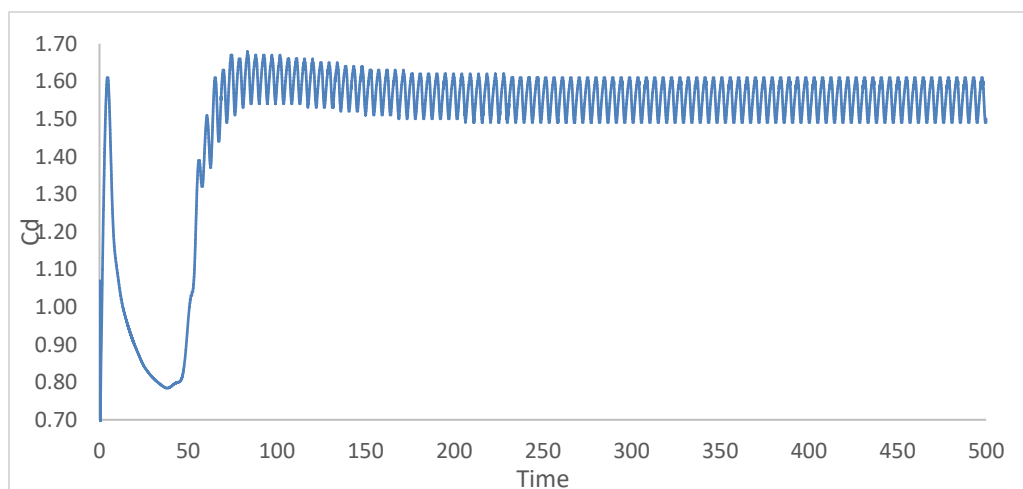


Figure 11: Drag coefficient Case A

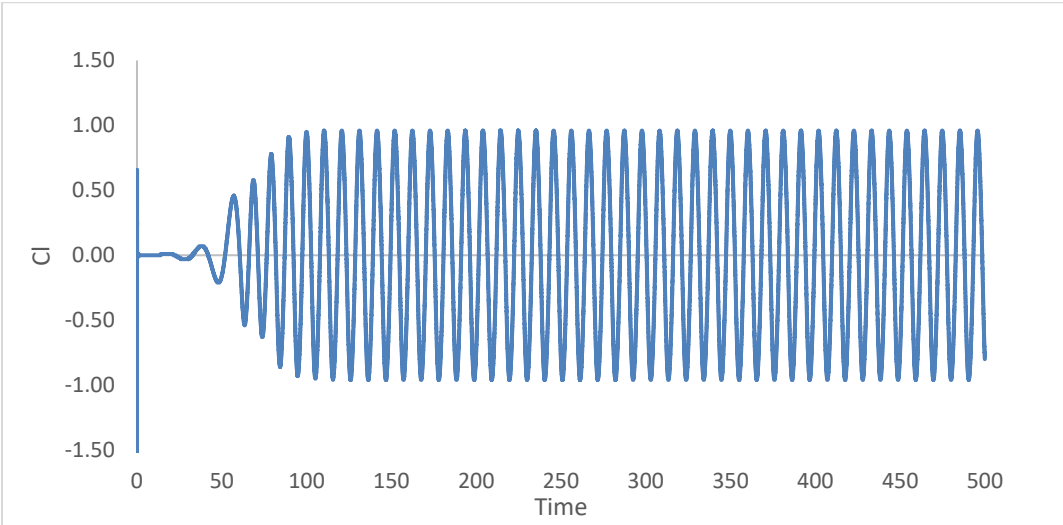


Figure 12: Lift coefficient Case B

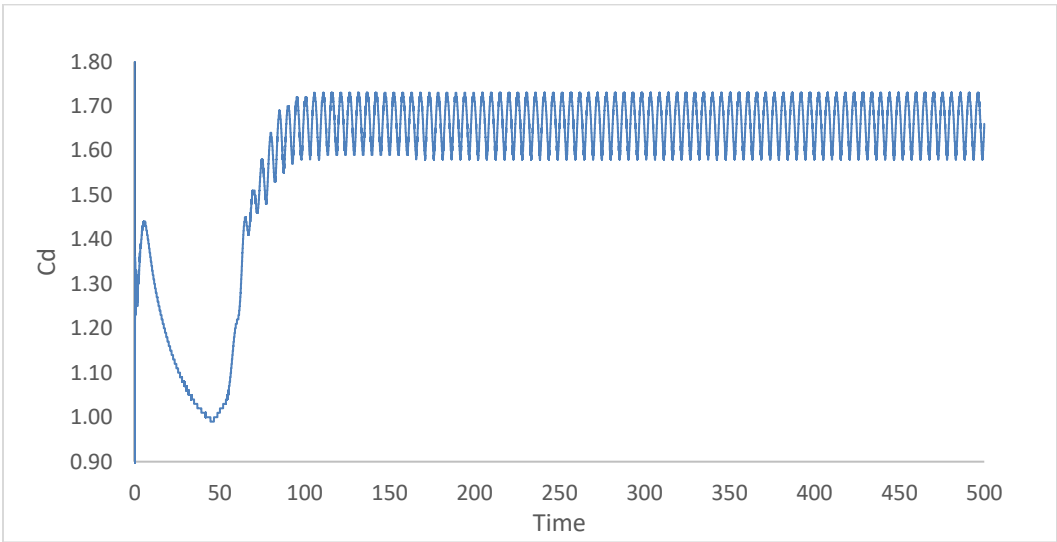


Figure 13: Drag coefficient Case B

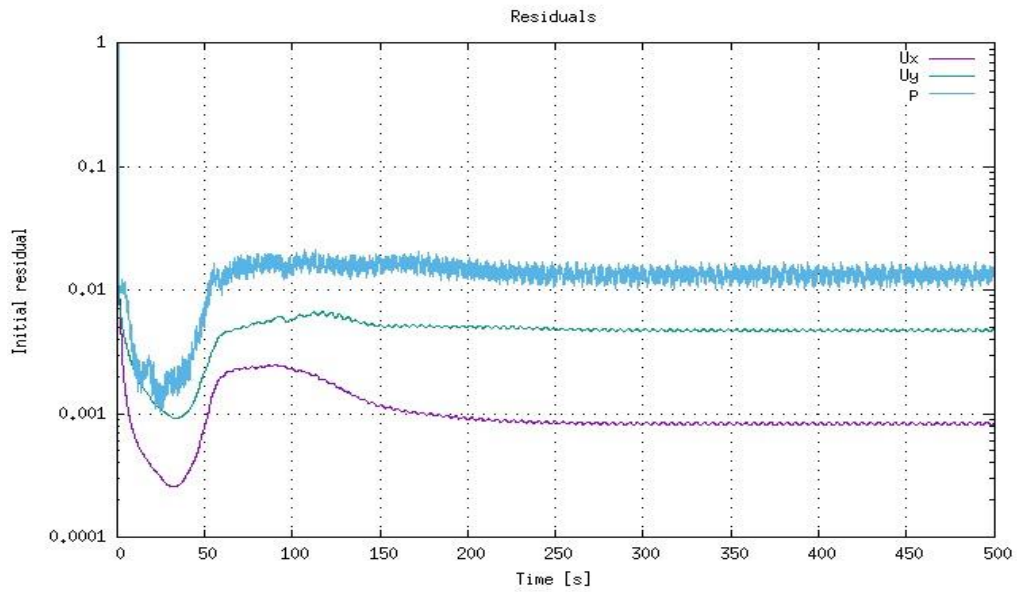


Figure 14: Residuals convergence case A

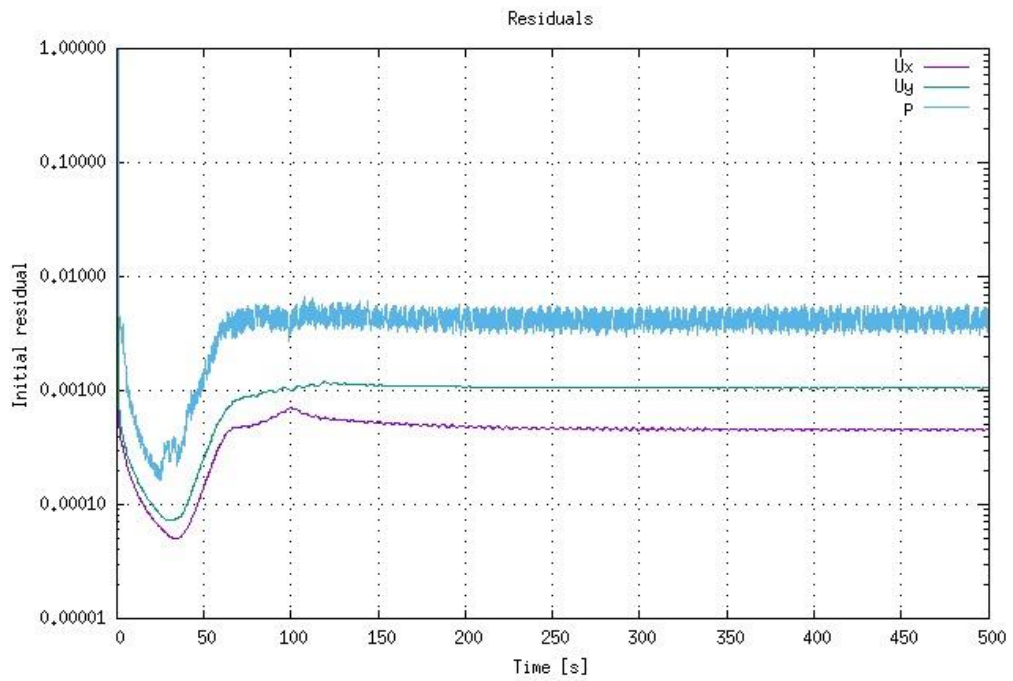


Figure 15: Residuals convergence case B

## 5 Comparison and validation

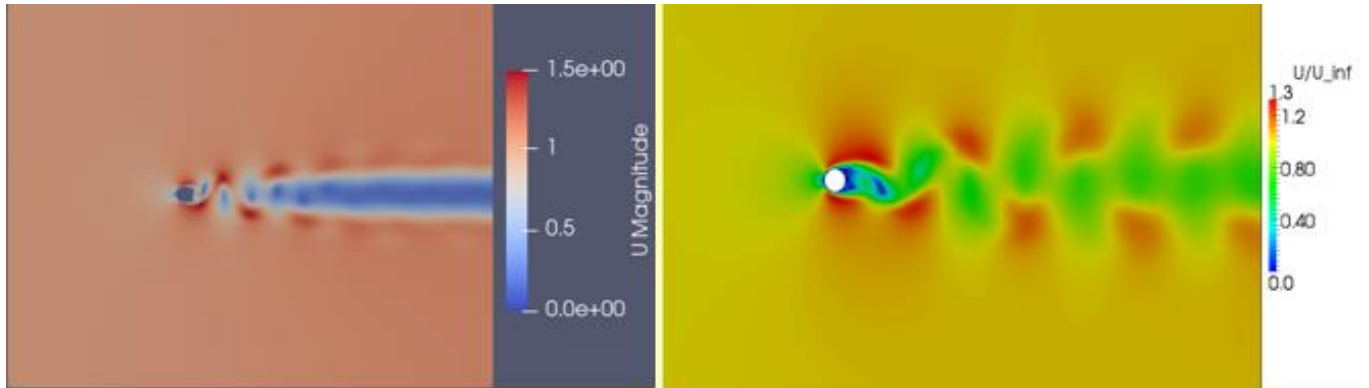


Figure 16: Simulation results & research paper U Magnitude case A

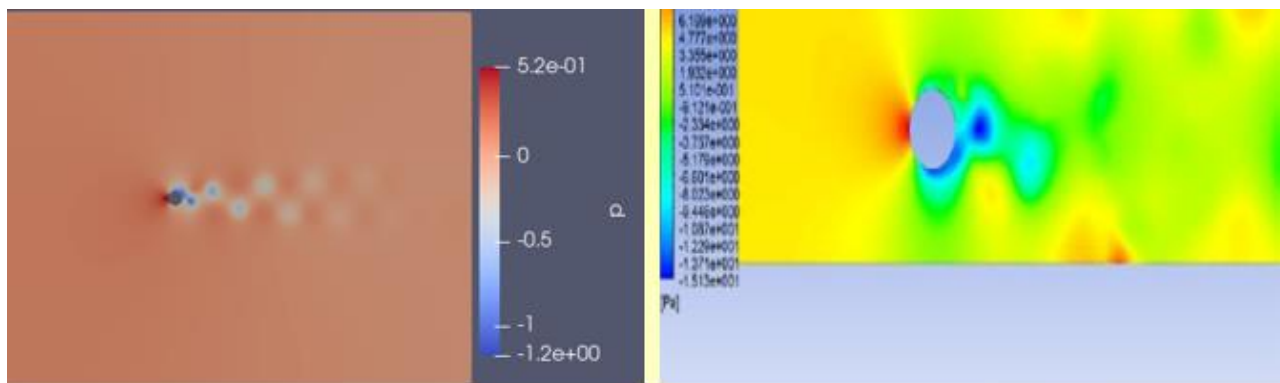


Figure 17: Simulation results & research paper Pressure case A

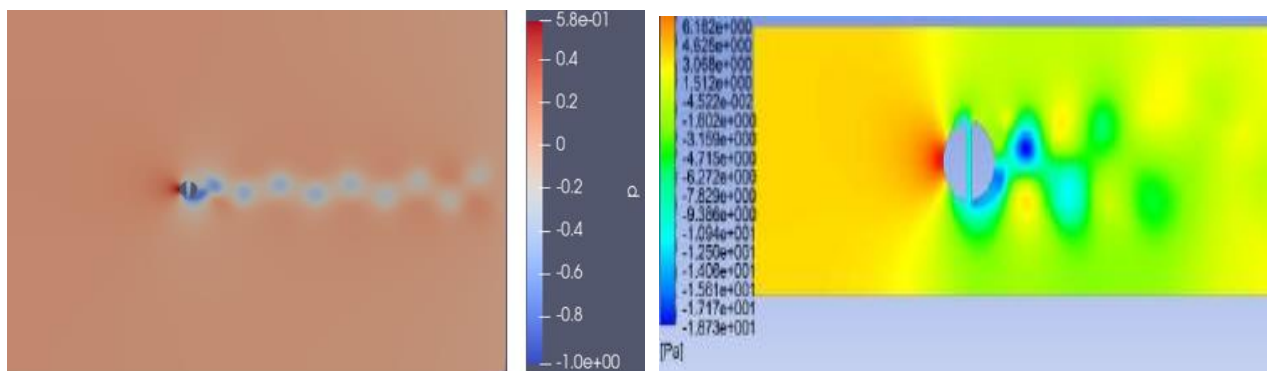


Figure 18: Simulation results & research paper Pressure case B

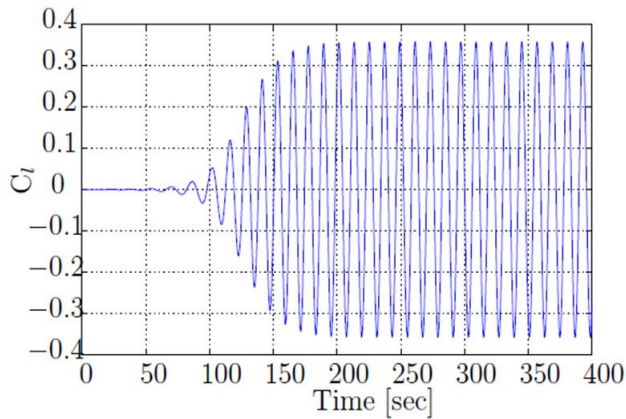


Figure 19: Research paper Lift coefficient

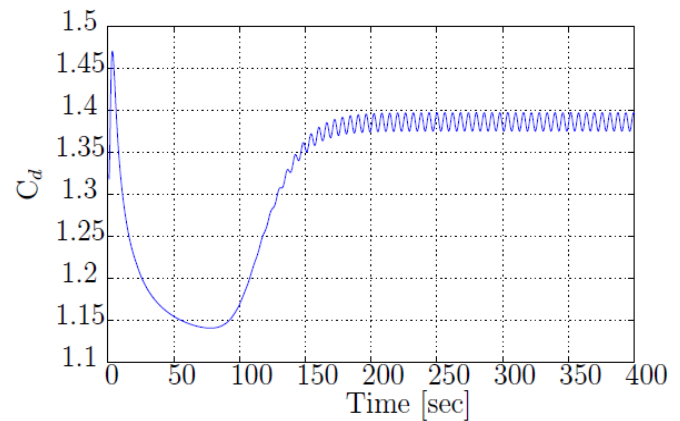


Figure 20: Research paper Drag coefficient

Validation of research paper lift and drag coefficient as shown in figure 19 and 20 comparison by simulation results of lift and drag coefficient as shown in figure 10,11,12 and 13. The U magnitude and Pressure comparison present in table2.

Table 2: Comparison and validation parameters

Parameters	Paper parameter	OpenFoam parameter
Velocity Magnitude A	0.0 – 1.3	0.0 – 1.5
Velocity Magnitude B	0.0 – 1.3	0.0 – 1.4
Pressure A	-1.5 – 6.1	-1.2 – 5.7
Pressure B	-1.8 – 6.1	-1.0 – 5.8
Lift coefficient A	0.4	1.00
Lift coefficient B	0.4	0.9
Drag coefficient A	1.4	1.65
Drag coefficient B	1.4	1.7

## References

- [1] Sumer, B. Mutlu, et al. Hydrodynamics Around Cylindrical Structures. Singapore:World Scientific, 2006
- [2] Fox, Robert W., et al. Introduction to Fluid Mechanics. Hoboken, NJ: Wiley, 2010
- [3] Durbin, Paul A., et al. Fluid Dynamics with a Computational Perspective. Cambridge Cambridge Univ. Press, 2007
- [4] L. Euler, “Principes generaux du mouvement des fluids”, Histoire de l’Academie Royale des Sciences et te Belles Lettres,. Memoires de l’Academie Royale des Sciences et le Belles Lettres, vol. XI, pp. 274-315,1755.
- [5] M. Navier, “Memoire sur les lois du mouvement fluids”, Memoire de l’Academie Royale des Sciences de l’Institut de France, vol. VI, pp. 389-440, 1823.
- [6] G.G. Stokes, “On the theories of the internal friction of fluids in motion, and of the equilibrium and motion of elastic fluids”, Transactions of the Cambridge Philosophical Society, vol. VIII, p. 287,1845
- [7] T. Cousins, S.A. Foster, and P.A. Johnson, “A linear and accurate flowmeter using vortex shedding”, in Proc. Power Fluid for Process Control Symposium, Inst. Measurement and Control, Guildford, UK, 1975, pp. 45-46.
- [8] R.W. Miller, J.P. De Carlo, and J.T. Cullen, “A vortex flowmeter – calibration results and application experience”, in Proc. Flow-Con, Brighton, 1977.
- [9] D.J. Lomas, “Vortex flow metering challenges the accepted techniques”, Control & Instrumentation (1975).
- [10] H.G. Kalkhof, “Influence of the bluff body shape on the measurement characteristics of vortex flowmeters”, in Proc